Chemosphere 146 (2016) 238–244

Contents lists available at ScienceDirect

Chemosphere

journal homepage: www.elsevier.com/locate/chemosphere

Seasonal variation of carbonaceous pollutants in $PM_{2.5}$ at an urban 'supersite' in Shanghai, China

Fengwen Wang [a, b, *], Zhigang Guo [c], Tian Lin [d], Neil L. Rose [e]

[a] State Key Laboratory of Coal Mine Disaster Dynamics and Control, Chongqing University, Chongqing 400030, China
[b] Department of Environmental Science, College of Resources and Environmental Science, Chongqing University, Chongqing 400030, China
[c] Shanghai Key Laboratory of Atmospheric Particle Pollution and Prevention, Center for Atmospheric Chemistry Study, Department of Environmental Science and Engineering, Fudan University, Shanghai 200433, China
[d] State Key Laboratory of Environmental Geochemistry, Institute of Geochemistry, Chinese Academy of Sciences, Guiyang 550002, China
[e] Environmental Change Research Centre, University College London, Gower Street, London WC1E 6BT, United Kingdom

HIGHLIGHTS

- An obvious seasonal variation of carbonaceous pollutants in $PM_{2.5}$ was observed.
- Petroleum residue contributed 71.4% to the *n*-alkanes.
- PCA analysis revealed mixed sources for the OC, EC and *n*-alkanes.
- Vehicle exhaust contributed more $PM_{2.5}$-bound hopanes than coal combustion.

ARTICLE INFO

Article history:
Received 7 September 2015
Received in revised form
4 December 2015
Accepted 9 December 2015
Available online 28 December 2015

Handling Editor: J. de Boer

Keywords:
Seasonal variation
Carbonaceous pollutants
$PM_{2.5}$
Shanghai

ABSTRACT

Multiple $PM_{2.5}$ samples collected through different seasons from October 2011 to August 2012 at an urban site in Shanghai, China were analyzed for carbonaceous pollutants. Data from this site, a 'super' air quality monitoring station at Fudan University, has been used by researchers to investigate the formation mechanism of haze episodes. The characteristics and concentrations of organic carbon (OC), elemental carbon (EC), *n*-alkanes, as well as relative abundances of hopanes, in these samples were determined. The concentrations showed a pronounced annual cycle with higher values in cold seasons (spring and winter, mean: 8.6 μg/m^3, 3.3 μg/m^3 and 136.4 ng/m^3 for OC, EC and *n*-alkanes, respectively) and lower values in warm seasons (fall and summer, mean: 6.6 μg/m^3, 2.6 μg/m^3 and 73.8 ng/m^3 for OC, EC and *n*-alkanes, respectively). EC generally displayed a common source with that of OC in all seasons. Petroleum residue was the major source of *n*-alkanes, contributing 71.4% to the targeted C_{14}–C_{33} *n*-alkanes over four seasons. Principal components analysis and the composition of hopanes showed that emissions from vehicle exhaust contributed more carbonaceous aerosols than coal combustion. These data could provide important information for measures to reduce carbonaceous pollutant emissions and improve air quality in Shanghai, and other urban centers across China.

© 2015 Elsevier Ltd. All rights reserved.

1. Introduction

$PM_{2.5}$ is particulate matter in the atmosphere with an aerodynamic equivalent diameter of 2.5 μm or less. It is a complex mixture of elemental and organic carbon, mineral dust, trace elements and water, and is known to produce respiratory and cardiovascular illness (Ha et al., 2014). Carbonaceous compounds can comprise a large but highly variable fraction of the $PM_{2.5}$ burden and may provide a better indicator of particulate substances harmful to human health than undifferentiated particle mass (Janssen et al., 2012). In general, these compounds can be classified as organic carbon (OC) and elemental carbon (EC). Organic carbon, formed by a variety of processes including primary emission and secondary conversion (e.g. by reaction with atmospheric gases), is an aggregate of organic compounds such as *n*-alkanes, aromatic and aliphatic compounds etc. Elemental carbon, sometimes also

* Corresponding author. State Key Laboratory of Coal Mine Disaster Dynamics and Control, Chongqing University, Chongqing 400030, China.
E-mail address: fengwenwang@cqu.edu.cn (F. Wang).

http://dx.doi.org/10.1016/j.chemosphere.2015.12.036
0045-6535/© 2015 Elsevier Ltd. All rights reserved.

known as black carbon (BC), is produced by the incomplete combustion of fossil fuels and biomass burning, as well as from the vapor phase as a condensation product. As a consequence EC (or BC) particles can range from graphite-like particles through to larger soot and chars (Rose and Ruppel, 2015). It has been demonstrated that these carbonaceous materials are associated with environmental, human health and climate effects (Jacobson, 2001; Menon et al., 2002; Kennedy, 2007) and as a consequence their sources, toxic effects, mass-balance budgets and their significance to biogeochemical cycles is receiving increased worldwide attention.

The impacts of carbonaceous compounds in aerosols on environmental and health effects are considered to be mostly associated with concentration, particle size and chemical compositions. *n*-Alkanes and hopanes are important components of carbonaceous compounds. *n*-Alkanes can be derived from both natural sources (e.g. higher plant waxes) and anthropogenic activities such as the combustion of diesel, gasoline and natural gas (Simoneit, 1986). Hopanes, markers for fossil-fuel emissions, are a group of organic compounds consisting of six isoprene units. Coal burning and engine exhausts are considered the potential main sources (Fraser et al., 1998). These pollutants, once emitted, are ubiquitous in environment and therefore can be used as markers for source identification of aerosols (Bi et al., 2002).

Shanghai, the largest Chinese city by population (nearly 24 million in 2013), is a global financial center, and a transport hub with the world's busiest container port. Located at the eastern end of the Yangtze River Delta (YRD) in east China, Shanghai has experienced rapid development in both urbanization and industrialization over recent decades. Due to its location at the center of the YRD, Shanghai has been, and continues to be, the focus of environmental pollutant studies in this region, especially of atmospheric organic pollution. For example, Yang et al. (2005) reported a one-year record of OC and EC in $PM_{2.5}$ in central Shanghai, and found an important contribution from biomass burning to the fine carbonaceous particle component. Gu et al. (2010) presented the occurrence and composition of polycyclic aromatic hydrocarbons (PAHs) based on over two years of $PM_{2.5}$ samples, revealing sources of petroleum and coal/biomass combustion. Similarly, Hou et al. (2011) investigated the characteristics and sources of OC and EC in $PM_{2.5}$ over 2006–2007, and assessed their role in heavy haze formation. These studies imply a significant role for carbonaceous pollutants in the composition of $PM_{2.5}$ in Shanghai and are supported by our previous research on source apportionment of PAHs in $PM_{2.5}$ (Wang et al., 2015).

Here, we focus on a detailed seasonal study of the characteristics of other organic compounds in $PM_{2.5}$ samples. This not only enhances our understanding of the pollution status and composition of carbonaceous pollutants in the fine particulate fraction in Shanghai but also provides significant new data on source apportionment and hence an important basis for human health studies in the city.

2. Materials and methods

2.1. Sampling site and sample collection

The sampling site (31.3° N, 121.5° E) is located on the roof of No 4. Teaching building at Fudan University (Huang et al., 2012). With many observation instruments on the roof, this site is a 'super' air quality monitoring station in Shanghai. Wujiao Chang shopping center, one of the four sub-centers in Shanghai, is approximately 1 km away. Two roadways with heavy traffic, Guoding Road and Handan Road, surround a major part of the campus. The resident population in this area (Yangpu District) is about 1.3 million (http://www.yprk.com/).

The $PM_{2.5}$ samples were collected on quartz filters (20 × 25 cm^2, 2600 QAT, PALL, USA) by an aerosol sampler at a flow rate of 18 m^3/h (Guangzhou Mingye Huanbao Technology Company). The samples were collected on a 23.5-h basis with a regular start at 09:00 and an end at 08:30 the following day. Four sampling campaigns, 24 Oct-16 Nov 2011 (fall, n = 20), 24 Dec 2011–11 Jan 2012 (winter, n = 18), 9–28 Apr 2012 (spring, n = 19) and 26 Jul-15 Aug 2012 (summer, n = 14), were conducted to represent four different seasons. A total of 71 samples were taken during the sampling period. Two parallel operational sample blanks (i.e., field blanks) were run and obtained for each season.

Before exposure, the quartz filters were wrapped in aluminum foil and combusted at 450 °C for 4 h in the muffle furnace to remove residual organic contaminants. Then they were put in a constant temperature and humidity chamber for at least 24 h and weighed using an analytical balance (model: Sartorius 2004 MP; reading precision: 10 mg) under stable temperature (20 ± 1 °C) and humidity (45 ± 5%). Each weighed filter was sealed in a marked valve bag and stored in a cool and dry condition before sample collection. After sampling, all the filters were re-weighed using the same analytical balance under the same temperature and humidity condition (i.e., 20 ± 1 °C, 45 ± 5%, at least 24 h) as pre-sampling filters to obtain sample mass concentrations. The weighed samples were then stored in a refrigerator until analysis.

2.2. Sample analysis for OC and EC

The OC and EC fractions in $PM_{2.5}$ samples were determined by the IMPROVE thermal/optical reflectance (TOR) method developed by the Desert Research Institute (DRI), Nevada, USA (Chow et al., 1993). A 0.544 cm^2 area of each sample was punched to analyze the targeted carbon fractions including four OC (OC1-OC4), three EC (EC1-EC3) sub-samples and a pyrolyzed carbon fraction (OP). OC1-OC4 were produced in a helium atmosphere at temperatures of 140 °C, 280 °C, 480 °C and 580 °C, respectively. EC1-EC3 were produced in a 2% oxygen/98% helium atmosphere at temperatures of 580 °C, 740 °C and 840 °C, respectively. OC was operationally defined as total carbon in the sample when heated to 550 °C in a 100% helium atmosphere. EC was defined as all carbon when heated to 800 °C in an atmosphere of 2% oxygen and 98% helium after removal of OC. OP was determined when a reflecting transmittance laser attained its original intensity after oxygen was added to the analysis atmosphere. OC and EC were obtained as OC1+OC2+OC3+OC4+OP and EC1+EC2+EC3-OP, respectively.

2.3. Sample analysis for n-alkanes

The analytical procedure for the measurement of *n*-alkanes was similar to that for PAHs (Wang et al., 2014). Half of each sample filter was used for Soxhlet extraction. The extraction lasted 48 h with dichloromethane (DCM) spiked with a mixture of 200 ng of deuterated phenanthrene (Phe-d_{10}, *m*/*z* 188) and deuterated chrysene (Chr-d_{12}, *m*/*z* 240) in order to determine the recovery rate. Sample extracts were concentrated to ~5 ml using a vacuum rotary evaporator at 40 °C, 50 rpm. Subsequently, the solvent was exchanged into *n*-hexane (HEX) and rotary evaporated to approximately 2 ml. The extracts were then transferred into 22-ml glass tubes and concentrated to ~2 ml under purified N_2. The concentrated extracts were sequentially cleaned in a chromatography column (8 mm in diameter) filled with 3 cm deactivated alumina (Al_2O_3: 1.53 g; mesh size: 100–200; supplier: Shanghai Guoyao Company), 3 cm silica gel (SiO_2: 1.20 g, mesh size: 80–100; supplier: Jiangsu Qiangsheng Chemical Company) and 1 cm anhydrous sodium sulfate (Na_2SO_4: analysis grade; supplier: Shanghai Dahe

Chemical Company), and eluted with 20 mL DCM/HEX (1:1, V:V). Prior to analysis for *n*-alkanes, the extracts were reduced to ~500 μL under a stream of purified N_2. A sample vial (2 mL) was prepared for the final concentrated extract, and hexamethylbenzene (HMB) was used as an internal standard to quantify the *n*-alkanes. All samples were injected with HMB and then concentrated to about 200 μL in preparation for GC–MS analysis. The GC-MSD (Agilent GC 6890 N coupled with 5975C MSD, equipped with DB5-MS column, 30 m × 0.25 mm × 0.25 μm) used helium as a carrier gas. The GC operating processing was: 60 °C for 2 min, ramped to 290 °C at 3 °C/min and held for 20 min. The sample was injected split-less with the injector temperature at 290 °C. The post-run time was 5 min with an oven temperature of 310 °C. Hopanes were analyzed under the same condition as *n*-alkanes. The concentration of *n*-alkanes was determined by using authentic standards of *n*-alkanes (C_{14}, C_{16}, C_{18}, C_{20}, C_{22}, C_{24}, C_{26}, C_{28}, C_{30} and C_{32}). Individual *n*-alkanes ($C_{14–33}$) were identified based on the retention times and mass spectra of target compounds against the authentic standards.

2.4. Sample analysis for hopanes

The extraction procedure and GC–MS analysis for hopanes was the same as for *n*-alkanes. Detection of hopanes was carried out by monitoring the respective typical ions: *m/z* 191 (Hu et al., 2009). Without authentic standard samples (i.e., reference material) of the targeted hopanes (Ts:18α(H)-22,29,30-trisnorneohopane; Tm:17α(H)-22,29,30-trisnorhopane; C29αβ:17α(H),21β(H)-norhopane; C29βα:17β(H),21α(H)-norhopane; C30αβ:17α(H),21β(H)-hopane; C30βα:17β(H),21α(H)-hopane; C31S:22S-17α(H),21β(H)-homohopane; C31R:22R-17α(H),21β(H)-homohopane; C32S:22S-17α(H),21β(H)-bishomohopane; C32R:22R-17α(H),21β(H)-bishomohopane), we can only present their relative abundances rather than concentration data.

2.5. QA/QC

The analyzer was calibrated with known quantities of sucrose. One replicate analysis was conducted for every ten samples. The difference determined from replicate analyses was less than 5% for TC (total carbon), and less than 6% for OC and EC. Two parallel blank filters were analyzed following the same procedures in each season. Results were corrected with respect to the average blank concentrations. Detection limits for the OC and EC were below 0.2 and 0.03 μg/m^3, respectively.

Organic reagents (DCM, HEX) used in extracting *n*-alkanes were purchased from Shanghai ANPEL Scientific Instrument Company (HPLC grade, purity: 95%). All vessels were first rinsed with hot potassium dichromate-sulfuric acid solution, then left overnight in the solution and washed using de-ionized water (18.2 MΩ Milli-Q water). After wrapping these vessels in aluminum foil, they were put in muffle furnace at 450 °C for 4 h. All utensils were rinsed twice with reagents before use. The QA/QC for *n*-alkanes was based on the recovery rate of Phe-d_{10} and Chr-d_{12}. These two species were assumed to have matched molecular weight and similar chemical properties to the targeted *n*-alkanes (Guo et al., 2009), which were those from $C_{14}H_{30}$ to $C_{33}H_{68}$. Nominal detection limits for individual *n*-alkanes ranged from 0.01 to 0.1 ng/m^3 according to the data sets reported by Kavouras et al. (1999) and Bi et al. (2002). The mean recoveries were 91% ± 13% for Phe-d_{10} and 103% ± 15% for Chr-d_{12}. Procedural blanks, standard-spiked blanks, and blank filters were analyzed, and all met QA/QC requirements. Sample results were calculated as blank corrected values by subtracting the average blank from each sample. Reported concentrations here were not recovery corrected.

3. Results and discussion

3.1. Concentrations of PM2.5 mass, OC, EC and n-alkanes

Average concentrations of $PM_{2.5}$ mass, OC, EC and associated *n*-alkanes in each season are shown in Table 1, and daily variations of OC, EC and *n*-alkanes during the sampling periods are plotted in Fig. 1. The concentrations of OC, EC, and *n*-alkanes in all $PM_{2.5}$ samples are shown in Table S1. $PM_{2.5}$ mass concentrations (μg/m^3) were highest in winter (104.3 ± 91.0) and lowest in summer (57.8 ± 27.9), with an annual average of 83.4 ± 58.9. Seasonal variations of OC and EC concentrations (μg/m^3) were similar to those of $PM_{2.5}$ mass, and varied from 5.3 ± 3.4 (summer) to 9.6 ± 5.4 (winter) and 2.0 ± 2.2 (summer) to 3.8 ± 2.9 (winter), respectively. OC and EC in $PM_{2.5}$ were well correlated ($R^2 = 0.86$), suggesting possible common sources. The percentage of TC (OC + EC) in $PM_{2.5}$ in fall, winter, spring, and summer was 12.1%, 13.8%, 12.0%, and 12.3%, respectively, with an annual mean of 12.6%.

Seasonal trends of *n*-alkanes during the sampling period are also plotted in Fig. 1. The average seasonal concentrations of *n*-alkanes in $PM_{2.5}$ (ng/m^3) were highest in spring (181.4 ± 100.9) and lowest in summer (62.5 ± 31.5), an approximate 3-fold difference. The carbon preference index (CPI) of *n*-alkanes has been used to identify the distribution of biogenic origins and anthropogenic materials (Simoneit, 1986). In this study, the CPI was calculated as the sum of the concentrations of the odd-carbon-number *n*-alkanes divided by the sum of the concentrations of the even-carbon-number *n*-alkanes, which is $CPI = \sum(C_{15}–C_{33})/\sum(C_{14}–C_{32})$. The relatively low values for the CPI (Simoneit et al., 1991) (1.5 in fall, 1.2 in winter, 1.8 in spring and 1.9 in summer; Table 1) indicate the importance of petroleum and diesel residues and gasoline emissions, as well as the lower contribution of *n*-alkanes emitted from epicuticular waxes. These results are consistent with those obtained by Feng et al. (2006). The maximum carbon number (C_{max}) in warm seasons (fall and summer) was C_{29}/C_{31}, while in cold seasons (winter and spring), it was C_{23}/C_{24}. A similar phenomenon was also observed in a previous study reported by Feng et al. (2006). Ambient temperature and source variation could both be important to the seasonal differences observed in this study.

Table 2 provides a comparison of concentrations of $PM_{2.5}$ mass, OC, EC and *n*-alkanes in Shanghai with those from some other areas of the world. These data indicate that $PM_{2.5}$ mass concentrations in Shanghai were lower than those detected in Xi'an by a factor of 1–2 (Wang et al., 2006), and are comparable with those in Beijing (He et al., 2006) and Guangzhou (Cao et al., 2003). However, compared with other cities in the world, such as Los Angeles (Minguillón et al., 2008), London, Porto and Vienna (Hamilton et al., 2002), the $PM_{2.5}$ mass concentrations in Shanghai were much higher. With regard to OC, EC and *n*-alkanes, concentrations in Shanghai were lower than those detected in Beijing, Guangzhou and Xi'an in China (Bi et al., 2003; Yang et al., 2005; Wang et al., 2006), comparable with those in London, Porto and Vienna, but higher than those reported for Los Angeles (Eiguren-Fernandez et al., 2004; Minguillón et al., 2008).

When compared with OC and EC data from previous reports for Shanghai, the levels of OC (in μg/m^3) in summer and fall in this study (average 6.6) were lower than the OC of 9.9 measured in 2002–2003, while EC was slightly lower: 2.6 and 2.9, respectively (Feng et al., 2006). The OC and EC levels (6.7 and 2.9, respectively) were also lower than those reported for 2005–2006 (16.1 and 3.0 respectively) (Feng et al., 2009). While compared with $PM_{2.5}$ from 2006 to 2007 (Hou et al., 2011) (7.4 and 2.8 EC, respectively), the OC and EC levels in this study didn't show statistically significant difference ($p > 0.05$). These data therefore suggest that the carbonaceous component of $PM_{2.5}$ in urban Shanghai has declined over the

Table 1
Average concentration of $PM_{2.5}$ mass, OC, EC, *n*-alkanes and associated indices.

	μg/m³					%	%	ng/m³	*n*-alkanes		
Season	$PM_{2.5}$	OC	EC	OC/EC	SOC	SOC/OC	TC/$PM_{2.5}$	yield *n*-alkanes	CPI	C_{max}	Waxed %
fall, 2011	80.6 ± 65.3	7.9 ± 8.7	3.1 ± 2.8	2.4	4.2 ± 5.5	46.5	12.1	85.0 ± 87.7	1.5	$C_{29/31}$	50.1
winter, 2011	104.3 ± 91.0	9.6 ± 5.4	3.8 ± 2.9	2.7	3.1 ± 1.6	36.2	13.8	91.4 ± 59.3	1.2	$C_{23/24}$	8.2
spring, 2012	89.6 ± 34.3	7.6 ± 2.8	2.7 ± 1.0	2.8	1.9 ± 1.6	23.7	12.0	181.4 ± 100.9	1.8	$C_{23/24}$	6.3
summer, 2012	57.8 ± 27.9	5.3 ± 3.4	2.0 ± 2.2	3.2	2.0 ± 0.8	43.7	12.3	62.5 ± 31.5	1.9	$C_{29/31}$	49.8

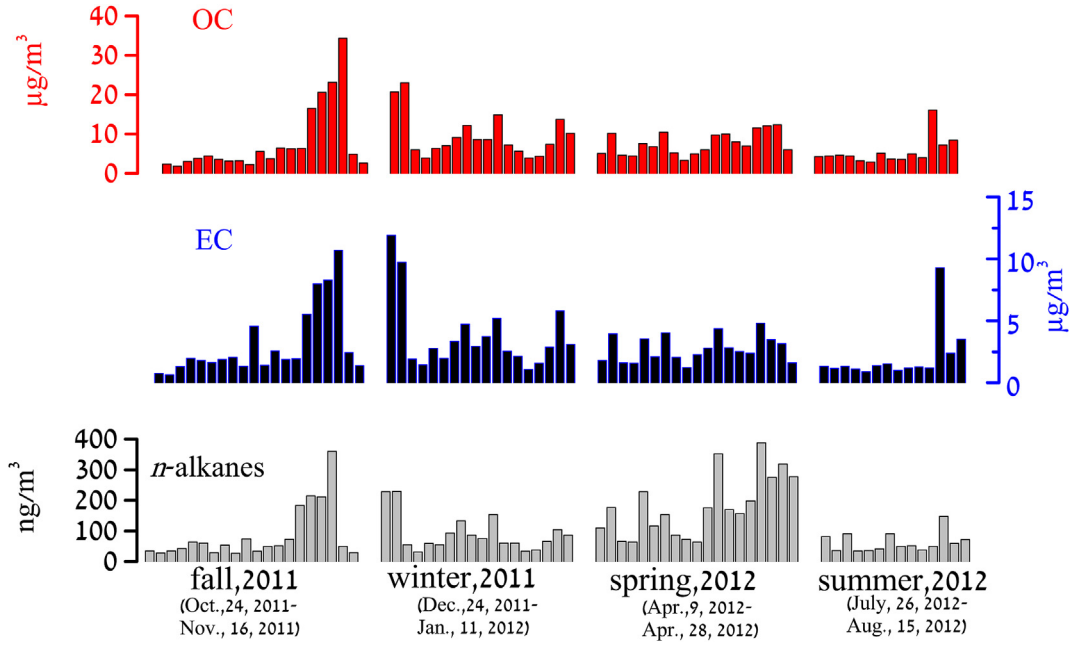

Fig. 1. Daily concentrations of OC, EC and associated *n*-alkanes over four seasons.

Table 2
Concentrations of $PM_{2.5}$ mass, OC, EC (μg/m³) and associated *n*-alkanes (ng/m³) for this study and studies in other cities around world.

Site	Period	Size	Mass	OC	EC	*n*-alkanes	References
Shanghai	2011,10–2012,08	$PM_{2.5}$	83.4	7.8	3.0	108.0	This work
Beijing	2002,07–2003,01	$PM_{2.5}$	73.7	26.2	–	220.5	He et al., 2006
Guangzhou	2002,01–2002,02	$PM_{2.5}$	105.9	22.6	8.3	–	Cao et al., 2003
Xi'an	2003,01–2003,07	$PM_{2.5}$	214.5	60.0	14.8	864.5	Wang et al., 2006
Los Angeles	2007,07–2007,09	$PM_{2.5}$	22.0	2.7	0.7	25.8	Minguillón et al., 2008
London	1995,09–1996,06	TSP	45.5	7.2	2.3	218.8	Hamilton et al., 2002
Porto	1995,09–1996,06	TSP	–	10.3	3.9	272.3	Hamilton et al., 2002
Vienna	1995,09–1996,06	TSP	–	11.5	3.4	188.3	Hamilton et al., 2002

past decade although the rate of this decline has slowed down in the last five years. However, despite these reductions, concentrations remain high and still indicate potential hazards to human health. Therefore, abatement strategies for carbonaceous aerosols associated with changes in the energy structure and industrial activities in the city need to be given more attention in the near future.

3.2. Secondary organic carbon (SOC) estimation and comparison

Estimates of secondary organic carbon (SOC) in $PM_{2.5}$ for Shanghai have previously been presented by Feng et al. (2009) and Hou et al. (2011), although these studies were conducted at different sites and estimated using different methods. Feng et al. (2009) applied the thermal-optical transmittance (TOT) method to measure OC and EC while Hou et al. (2011) used the TOR. In the present study, we provide an update on SOC concentrations and compare these datasets with those estimated by other researchers.

The OC/EC ratios in $PM_{2.5}$ were highest in summer (3.2), lowest in fall (2.4) and averaged over the year at 2.8. These results are comparable with those reported by Hou et al. (2011), in which the OC/EC was 3.5 and 2.2 in summer and winter, respectively. When compared with Feng et al. (2009), the OC/EC in our study was lower by a factor of 1–2 although it should be noted that OC/EC ratios measured by the TOT method are higher than values measured by TOR (Watson et al., 2005) and differences by a factor of two are common. Furthermore, Hou et al. (2011) conducted their sampling campaign at the same site as our current study while Feng et al. (2009) investigated suburban areas in the northwest of Shanghai. Therefore while it is difficult to draw direct comparisons between these studies, spatial variations across the city seem likely although uncertainties are high.

In our study, OC/EC ratios exceed 2.0, indicating SOC formation. The SOC was estimated by a common method that was introduced by Turpin (Turpin and Huntzicker, 1995) and developed by Castro (Castro et al., 1999). For a detailed description see Wang et al. (2015). Average seasonal SOC concentrations in $PM_{2.5}$ are listed in Table 1. High SOC concentrations ($\mu g/m^3$) in $PM_{2.5}$ were observed in fall (4.2) and winter (3.1), accounting for 46.5% and 36.2% of OC, respectively; while low SOC concentrations occurred in spring (1.9) and summer (2.0), accounting for 23.7% and 43.7% of OC, respectively. The lower contribution of SOC to OC occurred in spring and winter, which was consistent with that reported by Hou et al. (2011) (29.0% and 33.0% in spring and winter, respectively). In fall and summer, meteorological conditions, such as a higher frequency of sunny days and more intense solar radiation, could result in a higher photochemical activity (Castro et al., 1999). Therefore, higher SOC/OC in fall and summer could be due to the presence of precursors of semi-volatile organic compounds enhanced by favorable meteorological conditions. The seasonal trend of SOC in this study was similar to that reported for the Zha-bei district of Shanghai by Feng et al. (2009), which also displayed highest levels in the fall and lowest in the spring. Therefore, although our study was limited to a single site and cannot account for spatial variations of SOC in $PM_{2.5}$ across Shanghai, these data can provide a view of recent SOC pollution status and could be used by policy decision-makers to more effectively reduce carbonaceous pollutants.

3.3. Relationships between OC and EC, OC_{pri} and n-alkanes

The relationship between OC and EC can also indicate potential common sources and the correlations between the two for the four seasons are shown in Fig. 2. Strong correlations are observed over all four seasons: fall ($R^2 = 0.90$), winter ($R^2 = 0.97$), spring ($R^2 = 0.71$) and summer ($R^2 = 0.83$) suggesting common primary emission sources, such as vehicle exhaust, biomass burning and coal combustion. This result is in agreement with Feng et al. (2009), who showed that OC and EC undergo similar atmospheric dispersion processes and demonstrated the influence of both local sources and long range transport pathways.

According to Lim and Turpin, 2002, OC may be divided into two parts: primary OC (OC_{pri}) and secondary OC (OC_{sec}). OC_{pri} is emitted directly in particulate form from various emission sources (e.g., vehicular exhaust, fuel combustion), while OC_{sec} is formed through the gas/particle partitioning of semi- and nonvolatile products of chemical reactions involving reactive organic gases. The seasonal

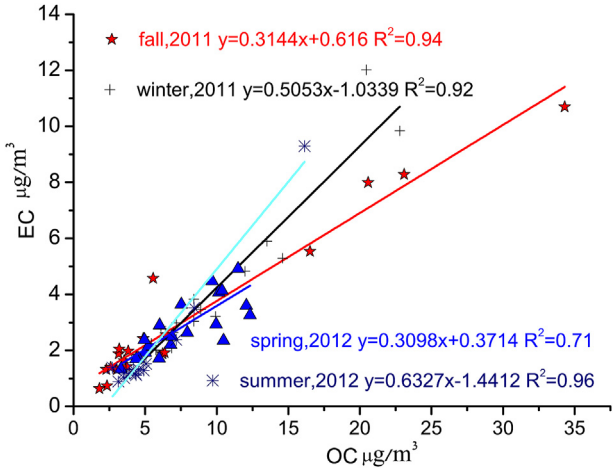

Fig. 2. Correlations between OC and EC on $PM_{2.5}$ for each season.

correlations between OC_{pri} and *n*-alkanes in $PM_{2.5}$ are shown in Fig. 3. Unlike the relationship between OC and EC, OC_{pri} and *n*-alkanes in fall and winter had higher correlations than those in spring and summer. The R^2 was 0.93 in fall and 0.92 in winter; while in spring and summer, it was 0.52 and 0.62, respectively. This indicates that more *n*-alkanes had a common source with that of OC_{pri} in fall and winter than in spring and summer. During the sampling period, C_{max} was C_{23} or C_{24} in spring and winter (Table 1) probably indicating gasoline as the dominant vehicle emission source (Schnelle-Kreis et al., 2005). In fall and summer, C_{29} or C_{31} dominated suggesting biogenic sources, especially epicuticular waxes from higher plants, were the predominant sources for these *n*-alkanes (Simoneit et al., 1991). According to Simoneit et al. (1991), *n*-alkanes can be divided into two source categories: plant wax and petroleum residue. Plant wax-derived *n*-alkanes can be calculated from the following equation:

$$\text{Wax } C_n = \frac{\left[Cn - \frac{(C_{n+1} + C_{n-1})}{2}\right]}{C_n}$$

The average contributions from plant waxes to *n*-alkanes over the four seasons are listed in Table 1. Plant waxes contributed more *n*-alkanes in fall and summer (average: 50.0%) than in spring and winter (average: 7.3%) probably due to biogenic activities, such as the abrasion of leaves and the transport of pollen. By contrast, in spring and winter, prevailing northwest winds bring anthropogenic pollutants via long-range transport from northern China (Wang et al., 2015), thus enhancing the contribution from petroleum residue.

3.4. Source identification of OC_{pri}, OC_{sec}, EC and n-alkanes using PCA

Principal component analysis (PCA) using SPSS 16.0 was performed on the datasets containing OC_{pri}, OC_{sec}, EC and 20 *n*-alkanes (C_{14}–C_{33}). The loadings for these variables on the three major principal components (PC1 – PC3) are shown in Table 3. These PCs explain 81.0% of the total variance (51.8%, 18.0% and 11.2%, respectively). PC1 had high loadings of C_{28}–C_{33} and moderate loadings of C_{16}–C_{17} and C_{24}–C_{25} *n*-alkanes, indicating a biogenic source (Simoneit et al., 1991) mixed with gasoline vehicle emission (Schnelle-Kreis et al., 2005). PC2 was characterized by high positive loadings of C_{18}–C_{23} *n*-alkanes and moderate loadings from OC_{pri}, EC, C_{17} and C_{24}. C_{21} indicates a diesel source (Schnelle-Kreis et al., 2005) and short chain *n*-alkanes mainly originate from petroleum residue. Therefore, PC2 was considered to be associated with sources from diesel and petroleum residue. PC3 was dominated by OC_{sec} and C_{26}–C_{27} with moderate loadings by EC and C_{32}–C_{33} *n*-alkanes. OC_{sec} is formed through atmospheric oxidation of volatile organic compounds and gas-to-particle conversion processes. EC mainly originated from anthropogenic activities and C_{26}–C_{33} *n*-alkanes were derived from higher plant wax. Thus, it is reasonable to infer that PC3 reflects a mixed source including anthropogenic fossil-fuel incomplete combustion and natural biogenic activity.

Based on the PCA analysis, the carbonaceous pollutants including OC_{pri}, OC_{sec}, EC and 20 *n*-alkanes were best explained by PC1 that was indicative of biogenic source and gasoline vehicle emission, and they also could be originated from diesel emission and petroleum residue.

3.5. Relative abundance of hopanes and source implication

Fig. 4 shows the distribution diagrams of hopane abundances relative to 18α(H)-22,29,30-trisnorneohopane (Ts: where Ts = 1)

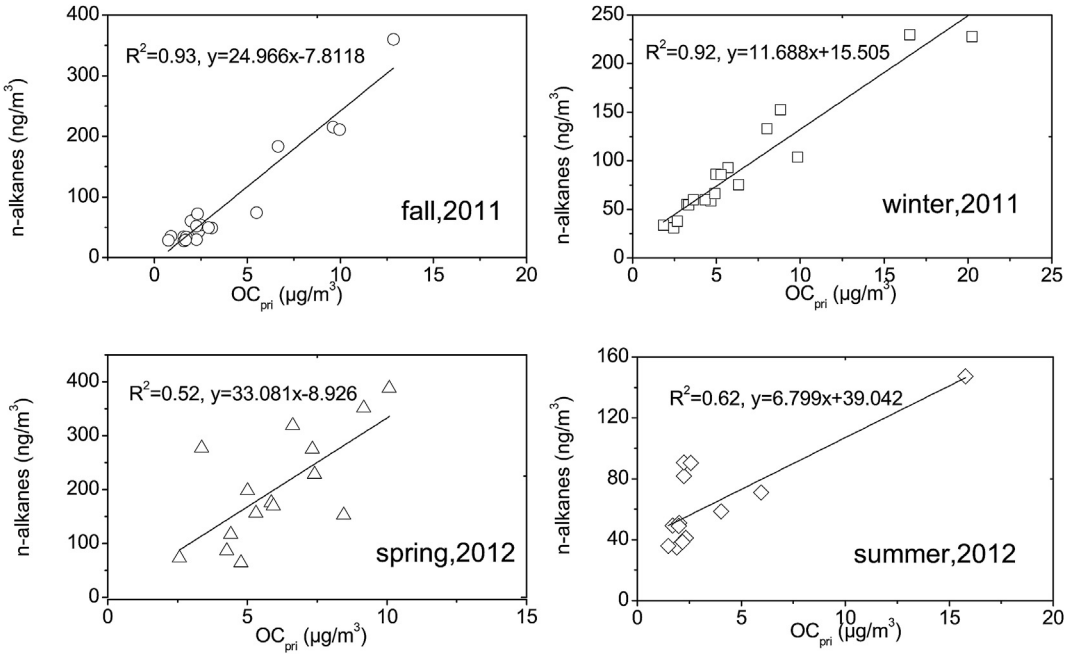

Fig. 3. Seasonal correlations between *n*-alkanes and OC_{pri}.

Table 3
Varimax rotated factor loading matrix of OC_{pri}, OC_{sec}, EC and *n*-alkanes in $PM_{2.5}$.

	PC1	PC2	PC3
OC_{pri}	0.383	**0.747**	0.384
OC_{sec}	0.152	–	**0.921**
EC	0.278	**0.624**	**0.615**
$C_{14}H_{30}$	0.049	–	0.023
$C_{15}H_{32}$	0.258	0.061	0.344
$C_{16}H_{34}$	**0.785**	0.140	–
$C_{17}H_{36}$	**0.615**	**0.610**	–
$C_{18}H_{38}$	0.387	**0.871**	0.013
$C_{19}H_{40}$	0.187	**0.937**	0.186
$C_{20}H_{42}$	0.037	**0.959**	0.185
$C_{21}H_{44}$	0.064	**0.958**	0.197
$C_{22}H_{46}$	0.119	**0.937**	0.243
$C_{23}H_{48}$	0.377	**0.831**	0.279
$C_{24}H_{50}$	**0.613**	0.581	0.210
$C_{25}H_{52}$	**0.851**	0.347	0.015
$C_{26}H_{54}$	0.037	0.386	**0.906**
$C_{27}H_{56}$	0.106	0.341	**0.915**
$C_{28}H_{58}$	**0.923**	0.166	0.144
$C_{29}H_{60}$	**0.870**	0.096	0.158
$C_{30}H_{62}$	**0.923**	0.083	0.191
$C_{31}H_{64}$	**0.910**	0.043	0.292
$C_{32}H_{66}$	**0.807**	0.130	0.499
$C_{33}H_{68}$	**0.762**	–	0.498
explained variance %	51.8	18.0	11.2

Middle and high values of the factor loading are boldfaced.

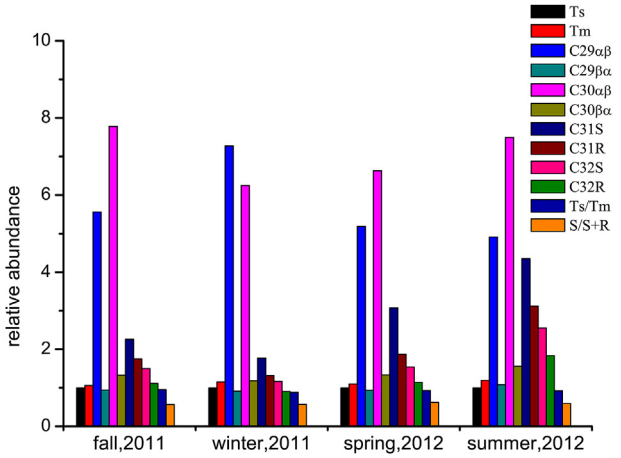

Fig. 4. Distribution diagrams of relative hopane abundances. (Ts:18α(H)-22,29,30-trisnorneohopane; Tm:17α(H)-22,29,30-trisnorhopane; C_{29}αβ:17α(H),21β(H)-norhopane; C_{29}βα:17β(H),21α(H)-norhopane; C_{30}αβ:17α(H),21β(H)-hopane; C_{30}βα:17β(H),21α(H)-hopane; C_{31}S:22S-17α(H),21β(H)-homohopane; C_{31}R:22R-17α(H),21β(H)-homohopane; C_{32}S:22S-17α(H),21β(H)-bishomohopane; C_{32}R:22R-17α(H),21β(H)-bishomohopane).

measured in each season. The seasonal distribution patterns of hopanes were all quite similar except in winter. When split seasonally, the most abundant compound in winter was 17α(H), 21β(H)-norhopane (C_{29}αβ), followed by 17α(H), 21β(H)-hopane (C_{30}αβ); while the other three seasons were dominated by C_{30}αβ with C_{29}αβ ranked second. C_{29}αβ is a tracer for motor vehicle exhaust (Schauer et al., 2002), providing evidence for a prominent contribution from this source in winter. The 18α(H)-22,29,30-trisnorneohopane/17α(H)-22,29,30-trisnorhopane ratio, abbreviated as Ts/Tm, ranged from 0.88 in winter to 0.95 in fall, with an annual average of 0.92. A Ts/Tm of 1.0 indicates a reduced impact from the combustion of less thermally mature fossil-fuels, such as biomass burning and coal combustion (Feng et al., 2005). The S/S + R, (the ratio of S- and R-isomers of 17α(H), 21β(H)-homohopane (C_{31}S and C_{31}R)), has been previously used to differentiate between coal burning and vehicle exhaust sources. In this study, the S/S + R ratio was in the range from 0.56 to 0.62, with a yearly average of 0.59 (Fig. 4), indicating a major contribution from traffic emissions (Fraser et al., 1998). Previous winter and summer data from 2002 to 2003, Feng et al. (2006) showed an S/S + R ratio in $PM_{2.5}$ in Shanghai of approximately 0.6, rather close to our results. Further study, both on the temporal and spatial scales and source contribution to aerosol-bound hopanes in Shanghai are needed. Detailed quantitative measurement for specific hopanes should prove to be an interesting and useful tracer.

4. Conclusions

An obvious seasonal variation in the concentrations and composition of carbonaceous pollutants was observed in $PM_{2.5}$ in urban Shanghai. The seasonal patterns for OC and EC were highest in winter and lowest in summer, similar to those previously reported by other researchers. On comparison with these earlier datasets, concentrations of OC and EC in 2011–2012 have declined over the past decade although the rate of decline has slowed over the latter five years. The ratio of SOC/OC remained higher in warm seasons (fall and summer) with respect to cold seasons (spring and winter), probably due to seasonal changes in emission sources and the corresponding prevailing meteorology. More *n*-alkanes had a common source with OC_{pri} in fall and winter than in spring and summer; while PCA revealed a mixture of sources including anthropogenic incomplete fossil-fuel combustion, petroleum residue and natural biogenic activity for the OC, EC and *n*-alkanes. Motor vehicle exhaust was a prominent contributor to the hopanes, especially in winter.

Acknowledgement

This work was supported by the National Natural Science Foundation of China (NSFC) (No: 21277030, 41176085, 41429501 (fund for collaboration with overseas scholars) and Hangzhou research project for environmental protection (2012001). We would like to thank Huaiyu Fu for the sample collection. We are grateful to the anonymous reviewers for their constructive comments which greatly improved this manuscript.

Appendix A. Supplementary data

Supplementary data related to this article can be found at http://dx.doi.org/10.1016/j.chemosphere.2015.12.036.

References

Bi, X., Sheng, G., Peng, P.A., Chen, Y., Zhang, Z., Fu, J., 2003. Distribution of particulate-and vapor-phase *n*-alkanes and polycyclic aromatic hydrocarbons in urban atmosphere of Guangzhou, China. Atmos. Environ. 37, 289–298.

Bi, X., Sheng, G., Zhang, Z., Fu, J., 2002. Extractable organic matter in PM10 from LiWan district of Guangzhou City. P. R. China. Sci. Total Environ. 300, 213–228.

Cao, J., Lee, S., Ho, K., Zou, S., Zhang, X., Pan, J., 2003. Spatial and seasonal distributions of atmospheric carbonaceous aerosols in Pearl River Delta Region, China. China Particuol. 1, 33–37.

Castro, L., Pio, C., Harrison, R.M., Smith, D., 1999. Carbonaceous aerosol in urban and rural European atmospheres: estimation of secondary organic carbon concentrations. Atmos. Environ. 33, 2771–2781.

Chow, J., Watson, J., Pritchett, L., Pierson, W., Frazier, C., Purcell, R., 1993. The DRI thermal/optical reflectance carbon analysis system: description, evaluation and applications in US air quality studies. Atmos. Environ. Part A. General Top. 27, 1185–1201.

Eiguren-Fernandez, A., Miguel, A., Froines, J., Thurairatnam, S., Avol, E., 2004. Seasonal and spatial variation of polycyclic aromatic hydrocarbons in vapor-phase and $PM_{2.5}$ in southern California urban and rural communities. Aerosol. Sci. Technol. 38, 447–455.

Feng, J., Chan, C., Fang, M., Hu, M., He, L., Tang, X., 2005. Impact of meteorology and energy structure on solvent extractable organic compounds of $PM_{2.5}$ in Beijing, China. Chemosphere 61, 623–632.

Feng, J., Chan, C., Fang, M., Hu, M., He, L., Tang, X., 2006. Characteristics of organic matter in $PM_{2.5}$ in Shanghai. Chemosphere 64, 1393–1400.

Feng, Y., Chen, Y., Guo, H., Zhi, G., Xiong, S., Li, J., Sheng, G., Fu, J., 2009. Characteristics of organic and elemental carbon in $PM_{2.5}$ samples in Shanghai, China. Atmos. Res. 92, 434–442.

Fraser, M., Cass, G., Simoneit, B., 1998. Gas-Phase and particle-phase organic compounds emitted from motor vehicle traffic in a Los Angeles roadway tunnel. Environ. Sci. Technol. 32, 2051–2060.

Guo, Z., Lin, T., Zhang, G., Hu, L., Zheng, M., 2009. Occurrence and sources of polycyclic aromatic hydrocarbons and *n*-alkanes in $PM_{2.5}$ in the roadside environment of a major city in China. J. Hazard. Mater 170, 888–894.

Gu, Z., Feng, J., Han, W., Li, L., Wu, M., Fu, J., Sheng, G., 2010. Diurnal variations of polycyclic aromatic hydrocarbons associated with $PM_{2.5}$ in Shanghai, China. J. Environ. Sci. 22, 389–396.

Ha, S., Hu, H., Roussos-Ross, D., Kan, H., Roth, J., Xu, X., 2014. The effects of air pollution on adverse birth outcomes. Environ. Res. 198–204.

Hamilton, R., Duarte, A., Kendall, M., Rocha-Santos, T., 2002. Airborne particle-associated polyaromatic Hydrocarbons, *n*-alkanes, elemental and organic carbon in three European Cities. J. Environ. Monit. 890–896.

He, L., Hu, M., Huang, X., Zhang, Y., Tang, X., 2006. Seasonal pollution characteristics of organic compounds in atmospheric fine particles in Beijing. Sci. Total Environ. 359, 167–176.

Hou, B., Zhuang, G., Zhang, R., Liu, T., Guo, Z., Chen, Y., 2011. The implication of carbonaceous aerosol to the formation of haze: revealed from the characteristics and sources of OC/EC over a mega-city in China. J. Haz. Mater. 190, 529–536.

Hu, L., Guo, Z., Feng, J., Yang, Z., Fang, M., 2009. Distributions and sources of bulk organic matter and aliphatic hydrocarbons in surface sediments of the Bohai Sea, China. Mar. Chem. 113, 197–211.

Huang, K., Zhuang, G., Lin, Y., Fu, J., Wang, Q., Liu, T., Zhang, R., Jiang, Y., Deng, C., Fu, Q., 2012. Typical types and formation mechanisms of haze in an eastern Asia megacity, Shanghai. Atmos. Chem. Phys. 12, 105–124.

Jacobson, M., 2001. Strong radiative heating due to the mixing state of black carbon in atmospheric aerosols. Nature 409, 695–697.

Janssen, N.A.H., Gerlofs-Nijland, M.E., Lanki, T., Salonen, R.O., Cassee, F., Hoek, G., Fischer, P., Brunekreef, B., Krzyzanowski, M., 2012. Health Effects of Black Carbon. World Health Organisation Regional Office for Europe, Copenhagen, 86pp.

Kennedy, I., 2007. The health effects of combustion-generated aerosols. In: Proceedings of the Combustion Institute 31 II, pp. 2757–2770.

Lim, H.J., Turpin, B.J., 2002. Origins of primary and secondary organic aerosol in Atlanta: results of time-resolved measurements during the Atlanta supersite Experiment. Environ. Sci. Technol. 36, 4489–4496.

Menon, S., Hansen, J., Nazarenko, L., Luo, Y., 2002. Climate effects of black carbon aerosols in China and India. Science 297, 2250–2253.

Minguillón, M., Arhami, M., Schauer, J., Sioutas, C., 2008. Seasonal and spatial variations of sources of fine and quasi-ultrafine particulate matter in neighborhoods near the Los Angeles-Long Beach harbor. Atmos. Environ. 42, 7317–7328.

Rose, N.L., Ruppel, M., 2015. Environmental archives of contaminant particles. In: Blais, J.M., Rosen, M.R., Smol, J.P. (Eds.), Environmental Contaminants: Using Natural Archives to Track Sources and Long-term Trends of Pollution. Developments in Paleoenvironmental Research Volume 18. Springer, Dordecht, pp. 187–221.

Schauer, J., Kleeman, M., Cass, G., Simoneit, B., 2002. Measurement of emissions from air pollution sources. 5. C_1-C_{32} organic compounds from gasoline-powered motor vehicles. Environ. Sci. Technol. 36, 1169–1180.

Schnelle-Kreis, J., Sklorz, M., Peters, A., Cyrys, J., Zimmermann, R., 2005. Analysis of particle-associated semi-volatile aromatic and aliphatic hydrocarbons in urban particulate matter on a daily basis. Atmos. Environ. 39, 7702–7714.

Simoneit, B., 1986. Characterization of organic constituents in aerosols in relation to their rigin and transport: a review. Int. J. Environ. Ana. Chem. 23, 207–237.

Simoneit, B., Sheng, G., Chen, X., Fu, J., Zhang, J., Xu, Y., 1991. Molecular marker study of extractable organic matter in aerosols from urban areas of China. Atmos. Environ. Part A. General Top. 25, 2111–2129.

Turpin, B., Huntzicker, J., 1995. Identification of secondary organic aerosol episodes and quantitation of primary and secondary organic aerosol concentrations during SCAQS. Atmos. Environ. 29, 3527–3544.

Wang, F., Lin, T., Feng, J., Fu, H., Guo, Z., 2015. Source apportionment of polycyclic aromatic hydrocarbons in $PM_{2.5}$ using positive matrix factorization modeling in Shanghai, China. Environ. Sci. Process. Impacts 17, 197–205.

Wang, F., Lin, T., Li, Y., Ji, T., Ma, C., Guo, Z., 2014. Sources of polycyclic aromatic hydrocarbons in $PM_{2.5}$ over the East China Sea, a downwind domain of east Asian continental outflow. Atmos. Environ. 92, 484–492.

Wang, G., Kawamura, K., Lee, S., Ho, K., Cao, J., 2006. Molecular, seasonal, and spatial distributions of organic aerosols from fourteen Chinese cities. Environ. Sci. Technol. 40, 4619–4625.

Watson, J., Chow, J., Chen, L., 2005. Summary of organic and elemental carbon/black carbon analysis methods and intercomparisons. Aerosol Air Qual. Res. 5, 65–102.

Yang, F., He, K., Ye, B., Chen, X., Cha, L., Cadle, S., Chan, T., Mulawa, P., 2005. One-year record of organic and elemental carbon in fine particles in downtown Beijing and Shanghai. Atmos. Chem. Phys. 5, 1449–1457.